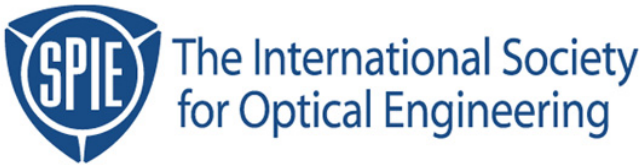

This paper was published in the proceedings of
Advances in Resist Technology and Processing XX, SPIE Vol. 5039, pp. 1143-1154.
It is made available as an electronic reprint with permission of SPIE.

Modeling Soft Bake Effects in Chemically Amplified Resists

Jeffrey Byers, Mark Smith, and Chris Mack
KLA-Tencor, 8834 North Capital of Texas Highway, Suite 301, Austin, Texas 78759, USA

John Biafore
Physical Simulation & Modeling, LLC

ABSTRACT

For lithography simulation physically correct resist models are required to achieve the best prediction of resist images across multiple process conditions. In the past, very limited work has been done to integrate the soft bake process into the full resist model. In this paper we describe how the soft-bake process generates a non-isotropic physical state in the resist. Then simple models for the effect of the solvent concentration, quencher concentration and free volume on the Exposure, PEB and develop kinetics are proposed and implemented. These models are coupled with the soft bake evaporation diffusion model to produce a physically based chemically amplified resist model that covers every processing step. The resulting model is used to simulate the kinetics for a chemically amplified resist as a function of soft bake condition.

Keywords: Chemically Amplified Resist, Soft Bake, Resist Simulation

1. INTRODUCTION

For lithography simulation physically correct resist models are required to achieve the best prediction of resist images across multiple process conditions. In the past, very limited work has been done to integrate the soft bake process into a physical resist model. The most popular approach has been to ignore the soft bake process entirely and treat the subsequent resist processing steps as independent of the soft bake conditions. One step higher on the evolutionary scale is to extract the resist parameters for exposure, Post apply bake (PAB) and develop models over a range of soft bake processes. The resist model parameters are then interpolated between this library of soft bake conditions. This approach may yield a composite resist model that works across a range of soft bake conditions but does not provide any insight into the underlying physical principles. Also the work required to implement such an approach is more than the average lithographer is willing to undertake. A physically-based coupling of the soft-bake process and the subsequent resist processing steps into a full resist model is desirable.

A significant amount of experimental work on characterizing the soft bake process has been published. This published work includes measurements of total solvent retention using mass spectrometry[1] C_{14} solvent tagging[2,3] quartz crystal microbalance[4], NMR [5], and ellipsometry[6,7]. The basic physical models for the soft bake step have been described in the literature. Various groups have presented models for the thermal decomposition, solvent evaporation and free volume limited diffusion[9] required to simulate the physical state of the resist after soft bake processing. These models describe the observed experimental data collected for the soft bake process and are a good starting point for coupling of the Soft Bake process into a full chemically amplified resist model.

In this paper we describe how the soft-bake process generates a non-isotropic physical state in the resist using the previously published evaporation-diffusion model. Then simple models for the effect of the solvent concentration, quencher concentration and free volume on the post exposure bake process are proposed and implemented. These models are coupled with the existing soft-bake model to produce a physicall-based resist model that predicts the soft bake influence on lithographic performance.

2. THEORY

Soft Bake Model

The soft bake process is a combination of solvent evaporation, solvent diffusion and polymer compaction, all of which are driven by the temperature profile of the soft bake process. Additionally, the resist additives may decompose, diffuse and evaporate during the soft bake step. A complete model for the solvent evaporation and solvent diffusion has been presented by Mack[9]. This model was used to fit the extensive collection of solvent retention and distribution collected by researchers at the University of Texas [3,4,9]. This solvent evaporation-diffusion model is explained below.

The solvent evaporation-diffusion process is represented by the partial differential equation.

$$\frac{dS(z)}{dt} = - k_{evap} \cdot S(z) \cdot \delta(z) + \nabla D_S \nabla S(z) \qquad (1)$$

in which S(z) is the solvent concentration as a function of depth into the resist, k_{evap} is the evaporation rate constant, and D_S is the solvent diffusion coefficient in the polymer film. The correct solution of Equation 1 is complicated by the non-constant diffusivity of small molecules such as solvent within polymer films. The solvent molecule itself plasticises the polymer film and enhances its own diffusivity. This non-Fickian diffusivity model is solvable only using numerical methods. For this work a 1D finite volume numerical solution of Equation 1 was implemented.

A free volume diffusivity model effectively describes the non-Fickian behavior of the solvent diffusivity in polymer films. In this model the diffusivity is controlled by the free volume, v_f , of the polymer. $D \propto e^{-\frac{B}{v_f}}$ (2)

Cohen and Turnbull[10] first proposed the free volume theory to describe diffusivity within solutions. About the same time, Williams, Landel and Ferry[11] described polymer relaxation kinetics for polymeric systems above the glass transition temperature , T_g, using a free volume expression. Later, Fujita et. al.[12] applied both models to describe the diffusivity of small molecules through polymer films. In this description of the polymer film, the free volume comes from both the increased thermal expansion of the polymer film above the glass transition temperature and the platicization volume from the added small molecules. Mack in his work[9] modified the free volume term to work above and below the polymer T_g. when solvent molecules are present in the film.

$$v_f = (1 - \chi_s) \cdot v_g + \alpha_2 \cdot (T - T_g) + \chi_s \cdot \beta \qquad (3)$$

where
χ_s = mass fraction of solvent
T_g = glass transition temperature of pure polymer
v_g = free volume of pure polymer at T_g
α_2 = differential thermal expansion coefficient above the T_g
β = density scaled fractional volume parameter

In this description of the free volume, the diffusivity can be written as

$$D = D_0 e^{-B\left(\frac{1}{v_f} - \frac{1}{v_g}\right)} \qquad v_f > v_g \qquad (4a)$$

$$D = D_0 \qquad v_f < v_g \qquad (4b)$$

where D_0 is the diffusion coefficient at T_g and B is the free volume efficiency parameter.

The evaporation term in Equation 1 can be derived from basic physical chemistry yielding a description of the evaporation rate constant k_{evap} in terms of basic thermodynamic properties of the solvent. The rate of material loss (kg per unit time) due to evaporation is proportional to the vapor pressure p_s (Newtons) of the evaporating material.

$$\frac{dm_S}{dt} = p_S \cdot \sqrt{\frac{M_S}{2\pi RT}} \tag{5}$$

In equation 5 M_s is the molecular weight of the evaporating material, T is the temperature (K), and R is the gas constant. Assuming the validity of Raoult's Law for the mixture, the vapor pressure of the solvent can be written as the product of the vapor pressure of the pure solvent and the solvent fraction at the polymer film surface.

$$p_S = p_s^0 \cdot \chi_S \tag{6}$$

Further, the vapor pressure of the pure solvent molecule as a function of temperature is described by the Claussius-Clapeyron equation

$$\frac{d\ln(p_s^0)}{d(1/T)} = -\frac{\Delta H_{vap}}{R} \tag{7}$$

where ΔH_{vap} is the heat of vaporization for the solvent. Assuming constant ΔH_{vap} over the range of temperature of interest the vapor pressure (atm) at any temperature can be related to the boiling point of the solvent since $p_s(T_{BP}) \equiv 1$ atm.

$$p_s^0 = e^{-\frac{\Delta H_{vap}}{R}\left(\frac{1}{T} - \frac{1}{T_{BP}}\right)} \tag{8}$$

Combining equations 5 through 8, the rate of solvent fraction change at the polymer surface due to evaporation can be written as

$$\frac{d\chi_S}{dt} = -6.249E^5 \cdot \sqrt{\frac{M_S}{RT}} \cdot e^{-\frac{\Delta H_{vap}}{R}\left(\frac{1}{T} - \frac{1}{T_{BP}}\right)} \cdot \chi_S \tag{9}$$

which yields the evaporate rate constant as a function of temperature

$$k_{evap} = 6.249E^5 \cdot \sqrt{\frac{M_S}{RT}} \cdot e^{-\frac{\Delta H_{vap}}{R}\left(\frac{1}{T} - \frac{1}{T_{BP}}\right)} \tag{10}$$

Equations 1, 3, 4 and 10 represent a complete model for solvent evaporation and diffusion during the soft bake process. It should be noted that the evaporation and diffusion of other resist components (e.g. base additives) can also be described using the same model. The free volume expression (Equation 3) must be summed over all components in the resist film.

$$v_f = (1 - \sum_i \chi_i) \cdot v_g + \alpha_2 \cdot (T - T_g) + \sum_i \chi_i \cdot \beta_i \tag{11}$$

The evaporation and diffusion of all components must be solved simultaneously using a coupled set of PDEs of the form given in Equation 1. The resulting concentration of solvent and resist additives as a function of depth into the resist can be incorporate into the post soft bake models (exposure, PEB and develop). In this paper we will discuss how the solvent and base concentration depth profiles affect the post exposure bake process.

Exposure Model.

Modeling the exposure step requires knowledge of the resist material bulk optical properties as well as the kinetics of the photochemical reaction. The bulk optical properties can be described entirely by the complex refractive index of the coated resist layer. The refractive index η is the sum of a real part n and imaginary part k. The refractive index of the resist film after soft bake can be approximated by a weighted average of the refractive index for each component in the film. This effective medium approximation can be written as

$$\eta_{resist} = (1 - \sum_i \chi_i) \cdot \eta_{polymer} + \sum_i \chi_i \cdot \eta_i \qquad (12)$$

where $\eta_{polymer}$ is the refractive index of the resist polymer, χ_i is the fraction of the ith resist component remaining after the soft bake step, and η_i is the complex refractive index of the ith component. The summation proceeds over all the non-polymer components of the resist film (solvent, PAG, base, etc.).

A kinetic description of the photochemical step can be ascertained from a simple first-order reaction mechanism of a photoacid generator (PAG) with the incident photons.

$$PAG + hv \xrightarrow{C} Acid$$

This mechanism can be described by a first order rate equation. The solution of this rate equation is typically written as a concentration of produced photoacid as a function of exposure dose in the resist film

$$[Acid] = [PAG]_0 - [PAG] = [PAG]_0 \cdot (1 - e^{-C \cdot Dose}) \qquad (13)$$

For this paper we assume that the exposure kinetic parameter C is unaffected by the soft bake process and that the final resist film refractive index and thickness are the main soft bake influences on the exposure step.

Post Exposure Bake Model

As with the exposure step, the PEB process can be described using a simple chemical mechanism. This mechanism is shown below and involves several concurrent reactions. First, the catalytic photoacid can react with polymer protecting sites, M, to generate deprotected sites, X, and to regenerate the catalytic acid. The photoacid can also react with base or quencher molecules, Q, within the resist to become an inactive species A-Q. This quenching reaction is an acid base equilibrium type reaction and should be reversible. These quencher molecules can come from unwanted contamination or can be purposely added to the resist to alter its lithographic performance. The acid molecule can also undergo other non-specific reactions that render it ineffective for catalysis. This later loss reaction is typically unknown and will be neglected for this work. A set of differential equations can be written to mathematically describe the time dependent concentration of each species represented in this mechanism. These are given in Equation 14. Because the concentration of species is not constant throughout the film and mass transport is possible, diffusion terms, e.g. $\nabla D \nabla$, are required for each species. The diffusion coefficients for both the photoacid and the base should be calculated using Equation 4 with the remaining solvent contributing to the free volume (Equation 11).

$$M + Acid \underset{\sigma D}{\overset{\sigma D}{\longleftrightarrow}} \{M - Acid\} \xrightarrow{k_a} X + Acid$$

$$Q + Acid \underset{k_{Q^-}}{\overset{k_{Q^+}}{\longleftrightarrow}} AQ$$

$$Acid \xrightarrow{k_{loss}}$$

$$\frac{dM}{dt} = -\frac{\sigma D \cdot k_a}{\sigma D + k_a} \cdot [Acid] \cdot [M] \tag{14a}$$

$$\frac{d[Acid]}{dt} = -k_{loss} \cdot [Acid] - k_{Q^+} \cdot [Acid] \cdot [Q] + k_{Q^-} \cdot [AQ] + \nabla D \nabla [Acid] \tag{14b}$$

$$\frac{d[Q]}{dt} = [Acid] - k_{Q^+} \cdot [Acid] \cdot [Q] + k_{Q^-} \cdot [AQ] + \nabla D_Q \nabla [Acid] \tag{14c}$$

$$X(t) = M_{t=0} - M(t) \tag{14d}$$

The bimolecular reaction between the protecting group and the acid is represented as a two-step reaction in which the two reactants must first come together and form a complex. This complex can either diffuse apart (the reverse reaction) or continue forward to produce the deprotected species and regenerate the catalytic acid. The complex formation and separation rates are diffusion limited and have the same rate constant, σD , where D is the diffusion coefficient of the acid molecule and σ is the cross-section number defining how close the two groups must be before reaction can take place. The forward reaction is controlled by a localized reaction rate constant k_a. The acid quenching reaction has both forward and reverse reaction rate constants. The ratio $K_{eq} = k_{Q^-} \big/ k_{Q^+}$ is the kinetic acid-base equilibrium constant for this acid-base pair in the polymer matrix at the associated PEB temperature.

It should be noted that the mechanism shown in Figure 3 is just one possible description for CAR resists. A less detailed mechanism can be used, in which the bimolecular reaction is represented by just one overall rate constant and assuming that the quenching reaction is assumed to be extremely fast and irreversible. This mechanism is

$$M + Acid \xrightarrow{k_a} X + Acid$$

$$Q + Acid \longrightarrow AQ$$

The rate equation for the protected group concentration is then

$$\frac{d[M]}{dt} = -k_a \cdot [Acid] \cdot [M] \tag{15}$$

where k_a is the overall rate constant for deprotection of the polymer. The functional form of the rate equation is the same for both mechanisms (Equations 14a and 15) , but Equation 14a distinguishes between diffusion limited and kinetic limited deprotection. If $\sigma D >> k_a$ then the overall rate reduces to k_a (kinetic limited). If $k_a >> \sigma D$ then the overall rate reduces to σD (diffusion limited). Classically, most bimolecular reactions in solid films are diffusion limited.

Develop Model

The develop step was modeled using a surface limited development in which the develop rate depends upon the localized extent of deprotection. There are many empirical models available for fitting this develop rate vs. deprotection function. None of the empirical models provide insight into the chemical origins of the develop function. They all should be interpreted as mere fitting functions and nothing more. The standard Mack model was used for the resist in this study. The standard Mack model functional form is shown in Equations 16a and 16b.

$$R_{Mack}(M) = R_{max} \cdot \frac{(a+1)\cdot(1-M)^n}{a+(1-M)^n} + R_{min} \tag{16a}$$

where

$$a = \frac{(n+1)}{(n-1)} \cdot (1 - m_{th})^n \tag{16b}$$

Most resists exhibit an apparent inhibition of develop rate at the top of the resist. A clear explanation of this inhibition for chemically amplified resists has not yet been established. For modeling purposes an exponential inhibition function was used in which the develop rate as a function of depth into the resist is modified as follows

$$R(z) = R(M) - R(M) \cdot R_{inh} \cdot \left(1 - e^{\frac{-z}{R_z}} \right) \tag{17}$$

where R(m) is the bulk develop rate calculated from either the Mack or Enhanced Mack models, z is the depth into the resist, R_{inh} is the inhibition factor, and R_z is the depth of inhibition. It is believed that the develop inhibition seen in chemically amplified resists is a function of the deprotection profile and as such should be modeled during the PEB process

3. ESTIMATING MODEL PARAMETERS

As described above, the free volume diffusion model required for the soft bake process has a large number of physical parameters. A common frustration for users of modeling software is the effort required to obtain simulation parameters. From a user perspective it is desirable to know the theoretical value and the physically significant range for each parameter. Theoretical values for most of the evaporation and diffusion parameters described in section 2 are discussed below.

First, the heat of vaporization can be estimated by noting that the entropy change going from the liquid to gas phase is fairly constant for most materials. At the boiling point the change in free energy for evaporation is zero and the resulting expression for ΔH_{vap} (cal/mol) is known as Trouton's rule

$$\Delta H_{vap} \approx 21.0 * T_{bp} \tag{18}$$

Table 1 shows the measured ΔH_{vap} and the Trouton's Rule value for several solvents. The agreement is fairly good. Since the boiling point and molecular weight of the solvent is easily obtained, the evaporation rate constant can be estimated using Equation 10.

Table 1: Boiling points and heats of vaporization for common resist solvent
For comparison, Trouton's Rule approximation is also listed.

Solvent	T_{bp} (°C)	ΔH_{vap} (kcal/mol)	Trouton's ΔH_{vap} (kcal/mol)
Water	100	9.72	7.85
Ethyl Lactate	145		8.79
PGMEA	154	10.39	8.98
Cyclohexanone	155	9.73	9.01

Williams-Landel and Ferry estimated values for α_2 and v_g as 0.00048 (K^{-1}) and 0.025 respectively. The exact value for α_2 should be easily measured using an ellipsometer. The relative thickness change with changing temperature defines the thermal expansion coefficient. α_2 is the difference in thermal expansion coefficient above the Tg and below the Tg. v_g is not so easily measured. However, published values for most polymer films have not varied significantly from the WLF value of 2.5%. This is especially true for the low molecular weight polymers common in photoresist systems.

The glass transition temperature , Tg, is seemingly easily measured. However, the thermal stability of many photoresist polymers is such that the standard method for determining the glass transition temperature has difficulty detecting the weak second order transition under the stronger thermal decomposition signal[6]. Values range from slightly lower than the soft bake temperature for annealing-type resists to approximately 80°C above the soft bake temperature for cycloolefin 193nm resists.

Cohen and Trunbull limit the B parameter to be within 0.5 and 1.0. Several researchers have reported values for B near 0.75. In this work the B value was fixed to the middle of the Cohen and Turnbull range (B=0.75).

D_0 and β parameters are diffusant/polymer dependent. Typical values can be estimated from published solvent retention data found in the literature. If the theoretical values for all other parameters are used and Tg is known then D_0 and β become the only adjustable parameters for this model.

4. RESULTS AND DISCUSSION

The resist used in this study was the Shipley KrF UV5 resist. This resist was chosen because it exhibits several key characteristics that can only be explained using a post exposure bake model coupled to the soft bake model. UV5 is reported to be of the ESCAP class of resist. ESCAP resists were developed to improve post exposure delay stability against environmental contamination from airborne amines. The deprotection kinetics and solvent retention data were measured using FTIR as a function of exposure dose, soft bake and post exposure bake condition. The methods used for data collection were previously published[13] and will not be discussed in detail here.

The solvent retention as a function of soft bake temperature was measured by tracking the absorbance peak for the carbonyl peak of the ethyl-lactate solvent. Since nothing else of significant concentration was assumed to evaporate during the soft bake the loss of carbonyl absorbance should be proportional to the loss of solvent. The concentration of remaining solvent can be obtained by scaling the carbonyl absorbance peak signal, A, using the formula

$$\chi_S = \chi_{initial} \frac{A_{initial} - A}{A_{initial} - A_0} \tag{19}$$

where $A_{initial}$ and A_0 are the peak signals for $\chi_{initial}$ and 0% solvent concentrations, respectively. One limitation of the method is that the values for $\chi_{initial}$ and A_0 are difficult to obtain. In general A_0 can only be estimated from extremely long soft bake times. The value for $\chi_{initial}$ makes very little difference in the final solvent concentration[9] and only minor error results by fixing $\chi_{initial}$ at 20%.

The remaining solvent concentration for UV5 as a function of soft bake temperature was determined using the FTIR method and is shown in Figure 1. Ito and Sherwood published solvent retention results for a similar polymer system and several solvents. The Ito values are absolute solvent concentration obtained using NMR spectroscopy and do not have the scaling issue associated with our FTIR method. The Ito data is shown in Figure 1 for an ESCAP polymer and two solvents (Ethyl Lactate and PGMEA).

Using the solvent evaporation and diffusion model presented in Section II the total solvent content was calculated as a function of the soft bake temperature. The results are compared in Figure 1 with the experimental data. The simulation parameters used were the defaults presented in Section III with the exception of Tg and β. Tg was fixed at 135°C. The β parameter for each solvent was coarsely adjusted to match the experimental results. The β values used were β_{PGMEA} = 0.4, and $\beta_{Ethyl\ Lactate}$ = 0.7. PGMEA's lower utilization of the available free volume for diffusion (lower β value) is consistent with stronger solvent-polymer interaction through hydrogen bonding as reported by Ito. The Shipley UV5 resist shows a similar solvent retention curve as Ito's ESCAP with Ethyl Lactate.
Because the solvent evaporation comes from the top of the resist, the final solvent distribution within the resist will not be uniform. There will is always less solvent near the top of the resist than at the bottom. The magnitude of solvent non-uniformity is controlled by the various model parameters and process conditions. Figure 2 shows the simulated solvent concentration as a function of depth into the resist for UV5. The process conditions were 130°C and 140°C. This solvent distribution leads to important vertical differences in the resist.

The same free volume diffusivity model that applies to solvent should also apply to the other diffusing compounds with a resist film. Because of the ability of solvent to enhance diffusivity by increasing the free volume (Equation 4), the diffusion coefficient of the photoacid (and the base) is determined by how much solvent remains after the soft bake. If the solvent concentration varies with depth into the resist, the diffusion coefficient of the photoacid (and base) should also vary with depth into the resist. The calculated photoacid diffusivity as a function of depth into the resist is shown in Figure 2 for UV5 after 130 and 140°C soft bakes. To calculate the diffusivity of photoacid as a function of free volume shown in Figure 2 we set the β_{acid} to 0.23 and leave the other diffusivity model parameters the same as for the solvent. As shown in Figure 2 the diffusivity of the photoacid is predicted to be remarkably larger near the bottom of the resist than at the top. The gradient in diffusivity extends over 200 nm into the photoresist. Likewise, the average diffusivity after the higher soft bake condition (D_{140} = 9.6 nm^2/s) is 6 times lower than after the lower soft bake condition (D_{130} = 57 nm^2/s) . This diffusivity variation with depth and soft bake temperature can produce large resist performance and profile changes with soft bake temperature.

The kinetics of the PEB process are also influenced by the soft bake process. The kinetics are described by Equations 14a-14d. To determine the influence of the soft bake process conditions on the PEB kinetic parameters for UV5, the protection group concentration as a function of exposure dose was measured for 5 different soft bake conditions. The experimental results are shown in Figure 3. These plots are called chemical contrast curves[14]. By fitting these chemical contrast curves the PEB kinetic parameters can be obtained. The chemical contrast curves for chemically amplified resists typically have three distinct regions. The low exposure dose range shows little if any change in the protecting group until a threshold dose is reached. Above the threshold dose, the protection group concentration drops off quickly with increasing exposure dose. At very high doses the protection group concentration levels off asymptotically with increasing exposure dose. The limited deprotection at exposure doses below the threshold dose is a direct consequence of photoacid quenching by the added base. Once the photogenerated acid titrates the added base, deprotection becomes significant.

With UV5 the threshold exposure dose decreases with increasing soft bake temperature. This may be a consequence of base evaporation during the soft bake process. To investigate this theory, base evaporation and diffusion during the soft bake was simulated. The evaporation and diffusion model for base is the same as for the solvent. Using our Finite-

Volume solver the solvent evaporation and base evaporation were computed simultaneously since the solvent concentration contributes significantly to the free volume of the polymer and controls the base diffusion during the soft bake. The final base concentration profile after soft bake was then fed into the PEB model as the initial base condition. Simulating the base evaporation required fitting the ΔH_{vap} for the base since the boiling point was not known. The β_{base} parameter was also fit and the initial base concentration was taken from the 100°C soft bake condition with the assumption that this soft bake condition had insignificant base evaporation. All other diffusion parameters were set to the same values as the solvent.

The rate of protecting group loss above the threshold exposure dose is proportional to the amplification rate constant k_a. As seen in Figure 3 this parameter appears to change with soft bake condition. This is not surprising since the diffusion coefficient for the photoacid depends upon soft bake condition and the deprotection reaction is diffusion limited. The amplification rate constant, and base evaporation parameters ΔH_{vap}, and β_{base} were fit by matching the chemical contrast curves for each soft bake condition. The simulated results (lines) are shown in Figure 3 compared with the experimental data (symbols). The final base evaporation parameters were $[Q]_{Initial}$=0.206 , ΔH_{vap}= 21.02kcal/mol, β_{base}=0.23. As shown in Figure 3 roughly 70% of the base evaporates at the highest soft bake condition investigated.

As mentioned earlier the photoacid diffusion coefficient varies dramatically with depth into the photoresist when the free volume diffusion model is used. This can lead to unusual profile shapes. UV5 for instance shows standing wave patterns near the top of the resist but not at the bottom when imaged on reflective substrates such as bare silicon. This is shown in cross-section of 250nm isolated lines in Figure 4. Using the modeling parameters extracted from the FTIR studies above the cross sectional profile was simulated and the results are also shown in Figure 4. The simulated resist profiles match fairly well. Although the profile shape does not exactly match the qualitative results of re-entrant profile shape and the unusual standing wave sidewall pattern are reproduced. This phenomenon is impossible to recreate without the incorporation of the soft bake model and solvent controlled PAG diffusion.

In match the chemical kinetics data, it was assumed that a single deprotection rate existed through the depth of the resist for each process condition. However, the deprotection rate varies with soft bake condition, which suggests that the deprotection rate depends upon the solvent concentration. One explanation is that the deprotection reaction is diffusion limited and is proportional to the diffusion coefficient.

5. CONCLUSION

In this paper existing soft bake models were coupled to the post exposure bake for chemically amplified resists. The solvent evaporation and free volume controlled diffusion model was used to simulate the soft bake process for the Shipley UV5 KrF resist. The soft bake condition was shown to influence the post exposure bake kinetics. This soft bake influence was effectively simulated by allowing base evaporation during the soft bake step and using a photoacid diffusion model that takes into account solvent induced free volume effects. The vertical dependence of the diffusion coefficient was shown to generate re-entrant resist profiles and inhibit standing wave removal at the top of the resist.

In future work the deprotection rate constant will be explicitly coupled to the diffusion constant, solvent evaporation during the post exposure bake will be included in the model, and the influence of the solvent induced free volume on the develop model will be investigated.

ACKNOWLEDGMENTS

The authors would like to thank John Petersen (Petersen Advanced Lithography) for providing the UV5 resist images and for his valuable discussions about the resist models presented in this paper.

REFERENCES

1. J.M. Shaw, M.A. Frisch, and F.H. Dill, IBM Journ. Res. Dev., **21**, (1977) pp219-226.
2. W.D. Hinsberg, S.A. MacDonald, C.D. Snyder, H. Ito, R.D. Allen, *ACS Symposium Series 537, Polymers for Microelectronic: Resists and Dielectrics*, American Chemical Society (1993) pp 101-110.
3. A.B. Gardiner, A. Qin, C.L. Henderson, S. Pancholi, W.J. Koros, C.G. Willson, R.R. Dammel, C.A.Mack, and W.D. Hinsberg, Diffusivity Measurements in Polymers Part II: Residual Casting Solvent Measurements by Liquid Scintillation Counting, Proc SPIE vol 3049 (1998) pp 850-860.
4. K.E. Mueller, W.J. Koros, Y.Y.Wang, C.G. Willson, Diffusivity Measurements in Polymers Part III: Quartz Crystal Microbalnce Techniques, Proc SPIE vol 3049 (1998) pp 871-878.
5. H. Ito, M. Sherwood, NMR Analysis of Chemically Amplified Resist Films, Proc SPIE vol 3049 (1998) pp 850-860.
6. P.J. Paniez, A. Vareille, P. Ballet, B. Mortini, Study of Bake Mechanisms by Real-Time In-Situ Ellipsometry, Proc SPIE vol 3333 (1998) pp 289-300.
7. S. D. Burns; M .D. Stewart; J. N. Hilfiker; R. A. Synowicki; G. M. Schmid; C. Brodsky; C. G. Willson; "Determining Free Volume Changes During the PEB and PAB of a chemically Amplified Resist." *Forefront of Lithographic Materials Research*, Proc. of the 12th International Conference on photopolymers, McAfee, New Jersey, U.S.A, 323-334 (2000).
8. C. A. Mack, D. P. DeWitt, B. K. Tsai, and G. Yetter, proc. SPIE , **2195**, 584 (1994).
9. C.A. Mack, Model Solvent Effects in Optical Lithography, PhD. Dissertation. University of Texas (1998).
10. M.H. Cohen, D. Turnbull, *J. Chem. Phys.* ,**31**, (1959), p 1164.
11. Williams, Landel, Ferry, J. American Chem. Soc., **77**, (1955) pp 3701-3706.
12. FujitaTransactions of the Faraday Soc., **56**, (1960) pp 424-437.
13. J.S. Petersen, J. Byers, and R. Carpio, International Conference on Micro- and Nano-Engineering, University of Glasglow, Scotland, 1996.
14. G.M. Wallraff, J. Opitz, G. Breyta, H. Ito, and B. Fuller, proc. SPIE , **2724** , 149 (1996).

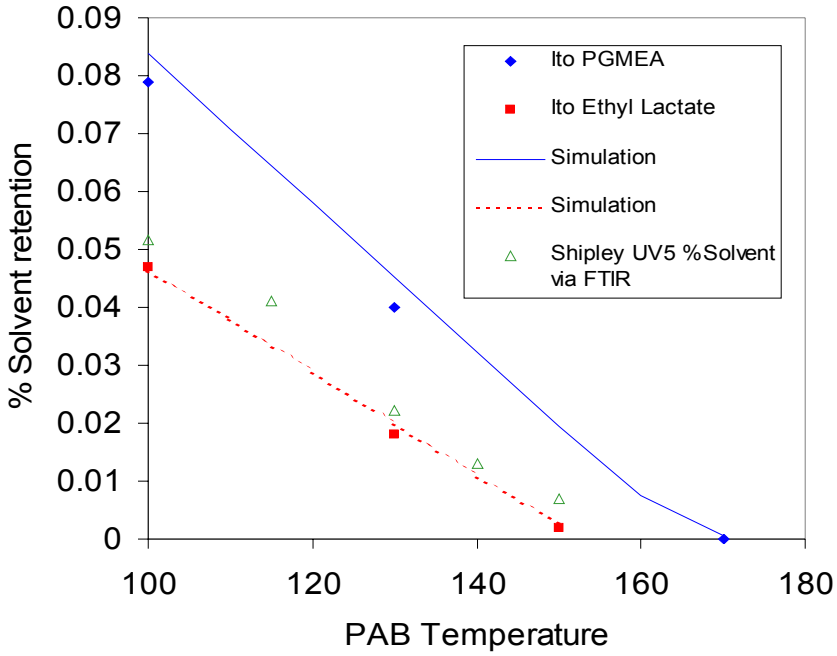

Figure1: Solvent concentration as a function of soft bake temperature for three polymer and solvent combinations. PGMEA (◆) and Ethyl Lactate(■) data taken from Ito[ref]. UV5 data (▲) measured using FTIR technique. Solvent for UV5 resist is ethyl lactate. For comparison simulations using evaporation-diffusion model are also shown.

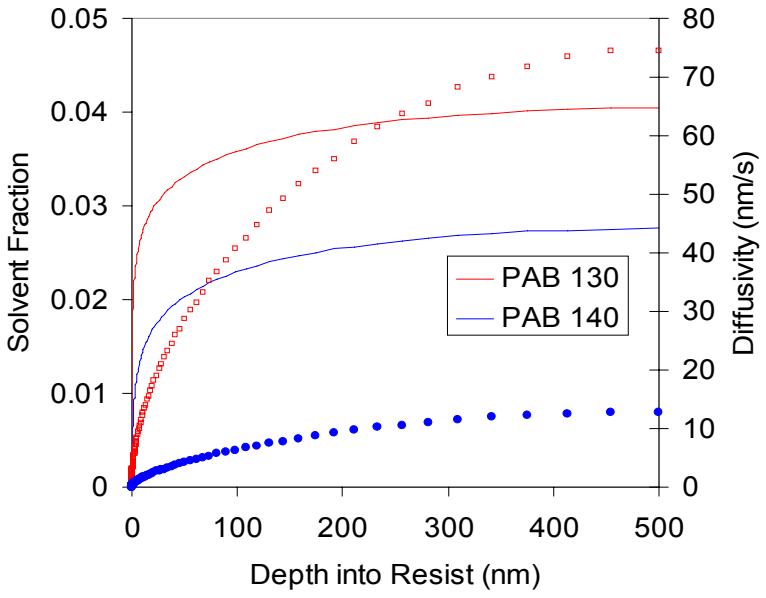

Figure 2: Graph of calculated solvent concentration as a function of depth into the resist (lines) for soft bakes temperatures below and above the polymer Tg. Also shown is the resulting estimated photoacid diffusion coefficient as a function of depth into the photoresist after the same two soft bake conditions.

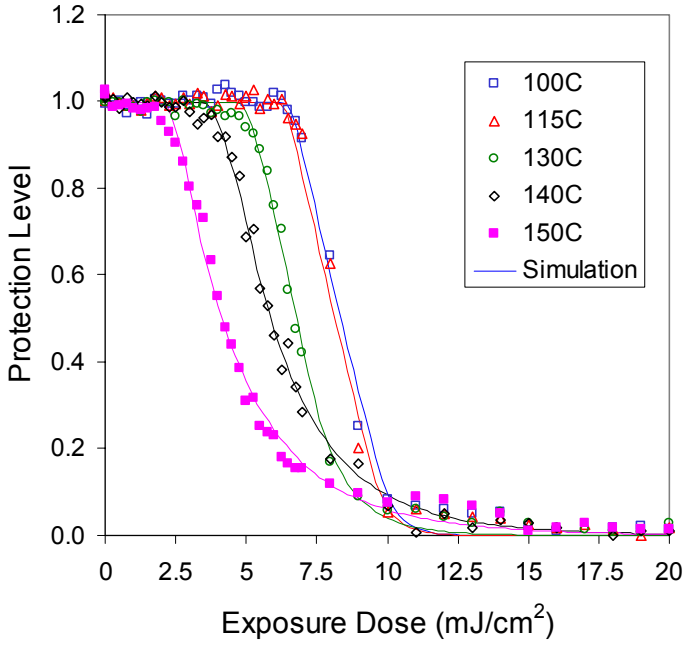

Figure 3: Graph of the protection level for UV5 as a function of exposure dose and soft bake temperature. Also shown is the comparison of the simulated result using the coupled soft bake model.

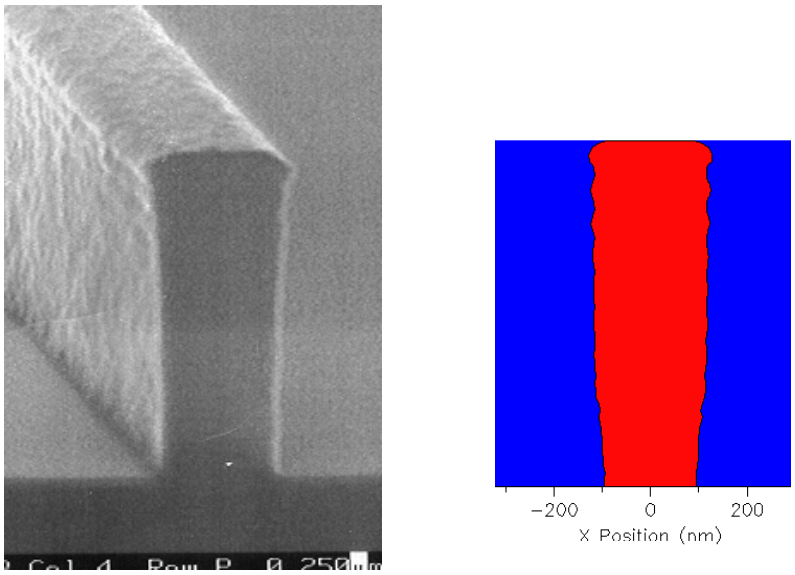

Figure 4: Experimental and simulated 250nm isolated line SEM images for Shipley UV5 Resist on silicon showing re-entrant profiles and standing at top of resist but not the bottom of the resist.